

# Nature of finite-temperature transition in anisotropic pyrochlore $\text{Er}_2\text{Ti}_2\text{O}_7$

M. E. Zhitomirsky,<sup>1</sup> P. C. W. Holdsworth,<sup>2</sup> and R. Moessner<sup>3</sup>

<sup>1</sup>*Service de Physique Statistique, Magnétisme et Supraconductivité,  
UMR-E9001 CEA-INAC/UJF, 17 rue des Martyrs, 38054 Grenoble Cedex 9, France*

<sup>2</sup>*Laboratoire de Physique, École Normale Supérieure de Lyon, CNRS 69364 Lyon Cedex 07, France*

<sup>3</sup>*Max-Planck-Institut für Physik komplexer Systeme, 01187 Dresden, Germany*

(Dated: February 20, 2014)

We study the finite-temperature transition in a model  $XY$  antiferromagnet on a pyrochlore lattice, which describes the pyrochlore material  $\text{Er}_2\text{Ti}_2\text{O}_7$ . The ordered magnetic structure selected by thermal fluctuations is six-fold degenerate. Nevertheless, our classical Monte Carlo simulations show that the critical behavior corresponds to the three-dimensional  $XY$  universality class. We determine an additional critical exponent  $\nu_6 = 0.75 > \nu$  characteristic of a dangerously irrelevant scaling variable. Persistent thermal fluctuations in the ordered phase are revealed in Monte Carlo simulations by the peculiar coexistence of Bragg peaks and diffuse magnetic scattering, the feature also observed in neutron diffraction experiments.

PACS numbers: 75.50.Ee,

*Introduction.*—Geometrically frustrated magnets are widely acknowledged for their exotic disordered states, which range from classical spin ice<sup>1</sup> to quantum spin liquids with fractionalized excitations.<sup>2–4</sup> Frustrated magnetic materials also feature various unusual types of order. An incomplete list of such states includes fractional magnetization plateaus,<sup>5–7</sup> a partially ordered state,<sup>8</sup> a valence bond solid,<sup>9</sup> and a quantum spin-nematic.<sup>10</sup> A recent example of unconventional magnetic order is provided by  $\text{Er}_2\text{Ti}_2\text{O}_7$ . This pyrochlore material undergoes a second-order transition at  $T_N \simeq 1.2$  K into a non-coplanar  $k = 0$  antiferromagnetic structure,<sup>11,12</sup> see Fig. 1(a). The peculiarity of this magnetic state stems from the fact that it appears to be stabilized by quantum and thermal fluctuations,<sup>13,14</sup> a phenomenon known as order by disorder. Despite intense theoretical and experimental studies of this and other closely related pyrochlore materials<sup>11–29</sup> a number of theoretical questions concerning  $\text{Er}_2\text{Ti}_2\text{O}_7$  remain tantalizingly open.

One pressing issue to be addressed in the present work is the nature of the transition at  $T_N$ . This is of interest both for the compound in question and as a general example of fluctuation driven ordering. The first Monte Carlo simulations on a local axis  $XY$  pyrochlore antiferromagnet found a fluctuation-induced first-order transition.<sup>15,16</sup> In our previous publication we have demonstrated that sufficiently strong anisotropic exchange interactions modify the transition to a continuous one. However, the precise critical behavior has not previously been studied. Experimental measurements<sup>11,23</sup> of the order parameter exponent  $\beta$  and the specific heat exponent  $\alpha$  indicate that the critical behavior of  $\text{Er}_2\text{Ti}_2\text{O}_7$  may be close to the three-dimensional (3D)  $XY$  universality class. In contrast, the ordered antiferromagnetic structure, Fig. 1(a), breaks only a discrete  $Z_6$  symmetry. The emergence of  $U(1)$  symmetry close to the transition point is not entirely surprising. Renormalization-group theory predicts that a  $Z_q$  anisotropy is dangerously irrelevant in 3D for  $q \geq 5$ .<sup>30,31</sup> From a numerical point of

view, the situation remains less clear. While early Monte Carlo results for a clock model<sup>32</sup> and an anisotropic  $XY$  model<sup>33</sup> generally confirm the scaling conclusions, two more recent studies of spin<sup>34</sup> and orbital<sup>35</sup> models with  $Z_6$  symmetry find values of the critical exponents  $\beta$  and  $\eta$  that are different from those of the 3D  $XY$  universality class. Thus, the critical behavior of models for  $\text{Er}_2\text{Ti}_2\text{O}_7$  needs to be clarified from a theoretical standpoint.

Another intriguing observation from neutron diffraction experiments<sup>17</sup> is the coexistence, below  $T_N$  and in zero magnetic field, of well-developed magnetic Bragg reflections and a broad diffuse scattering component. In the following we use large-scale Monte Carlo simulations to show that both the 3D  $XY$  universality of the transition and the coexistence of ordered and disordered components in the magnetic neutron scattering can be naturally understood and explained in the framework of our minimal spin model for  $\text{Er}_2\text{Ti}_2\text{O}_7$ . They also add a new twist to the story of a dangerously irrelevant anisotropy in the 3D  $XY$  model.

*Model.*—The low-temperature magnetic properties of  $\text{Er}_2\text{Ti}_2\text{O}_7$  and a number of other pyrochlore materials are adequately represented by an effective model of interacting Kramers doublets selected by a strong crystalline electrical field.<sup>20,21</sup> The control parameter for this approximation is a ratio of the exchange interaction  $J \sim 0.1$  meV to the crystal-field gap  $\Delta \sim 6$  meV.<sup>11</sup> The resulting pseudo-spin-1/2 Hamiltonian contains only the bilinear terms that are allowed by the crystal lattice symmetry.<sup>36</sup> Several equivalent representations have been used for this effective Hamiltonian. Below we use a convenient vector representation:

$$\hat{\mathcal{H}} = \sum_{\langle ij \rangle} \left\{ J_{zz} S_i^z S_j^z + J_{\perp} \mathbf{S}_i^{\perp} \cdot \mathbf{S}_j^{\perp} + J_{\perp}^a (\mathbf{S}_i^{\perp} \cdot \hat{\mathbf{r}}_{ij}) (\mathbf{S}_j^{\perp} \cdot \hat{\mathbf{r}}_{ij}) + J_{z\perp} [S_j^z (\mathbf{S}_i^{\perp} \cdot \hat{\mathbf{r}}_{ij}) + S_i^z (\mathbf{S}_j^{\perp} \cdot \hat{\mathbf{r}}_{ji})] \right\}. \quad (1)$$

Here  $S_i^z$  is a spin projection onto the local trigonal axis,

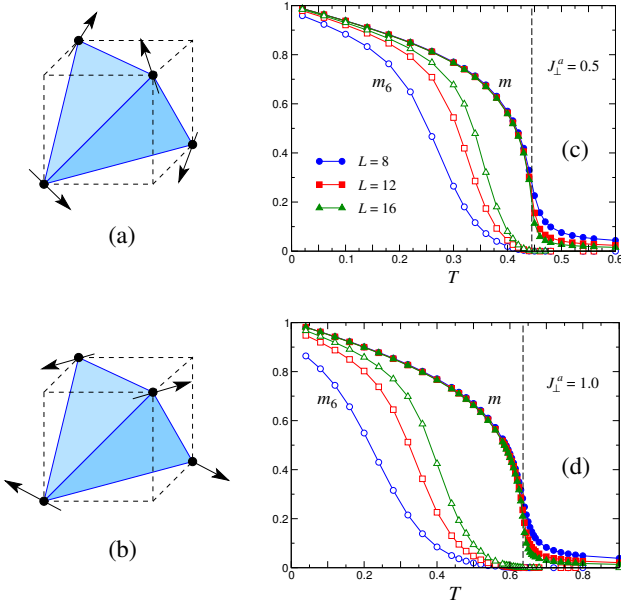


FIG. 1: (Color online) The noncoplanar magnetic structure of  $\text{Er}_2\text{Ti}_2\text{O}_7$ ,  $\psi_2$  state (a) and the coplanar  $\psi_3$  state (b). Panels (c) and (d) show the temperature dependence of two order parameters  $m$  (full symbols) and  $m_6$  (open symbols) for  $J_\perp^a = 0.5$  and  $J_\perp^a = 1$ , respectively.

$\mathbf{S}_i^\perp$  is the corresponding transverse component, and  $\hat{\mathbf{r}}_{ij}$  is a unit vector along the bond joining sites  $i$  and  $j$ . Savary *et al.*<sup>14</sup> used inelastic neutron scattering measurements in magnetic field to determine the exchange parameters corresponding to  $\text{Er}_2\text{Ti}_2\text{O}_7$ . Changing between the two sets of notations for coupling constants,<sup>37</sup> we obtain  $J_\perp = 0.21$ ,  $J_\perp^a = 0.35$ ,  $J_{zz} = -0.025$ ,  $J_{z\perp} = 0.03$  (all in meV). As  $J_{zz}$  and  $J_{z\perp}$  are small compared with the in-plane coupling constants, they can be safely neglected. As a result, one obtains the minimal model for  $\text{Er}_2\text{Ti}_2\text{O}_7$ , in which the anisotropic spin interaction are restricted to spin components lying in the local  $XY$  planes.

*Monte Carlo simulations.*—We perform Monte Carlo (MC) simulations of the classical model (1) with  $|\mathbf{S}_i| = 1$ ,  $J_{zz} = J_{z\perp} = 0$ , and  $J_\perp = 1$  and allowing local  $S_i^z$  fluctuations, *i.e.*, considering an effective  $XXZ$  model. The critical behavior is expected to be the same for classical and quantum models. Note that the high-temperature series expansion, the only other technique suitable for numerical investigation of anisotropic pyrochlores, gives a reasonably accurate estimate for  $T_c$  but has been so far unable to predict the critical properties.<sup>27</sup>

Our MC simulations were done for periodic clusters with  $N = 4L^3$  spins for various values of the control parameter  $J_\perp^a$ . We use Metropolis single spin-flip updates restricting the spin motion to increase the acceptance rate. In addition, micro-canonical over-relaxation steps were added to accelerate the random walk through phase space.<sup>38,39</sup> Typically a measurement was taken after 5 Metropolis steps, followed by 5 over-relaxation sweeps. This hybrid algorithm performs significantly better than

a plain Metropolis algorithm allowing us to simulate clusters up to  $L = 30$ . Statistical averages and the error bars were estimated by making 100 independent cooling runs.

The ordered magnetic state of  $\text{Er}_2\text{Ti}_2\text{O}_7$ ,  $[\psi_2]$ , Fig. 1(a)], transforms according to the two-component  $E$  ( $\Gamma_5$ ) irreducible representation of the tetrahedral point group  $T_d$ . A competing coplanar state  $\psi_3$  is shown in Fig. 1(b). The two states form a basis of the  $E$ -representation such that  $\psi_2 \sim (2z^2 - x^2 - y^2)$  and  $\psi_3 \sim (x^2 - y^2)$ . Accordingly, any lowest-energy spin configuration may be linearly decomposed into

$$m_x = \frac{1}{N} \sum_i \mathbf{S}_i \cdot \hat{\mathbf{x}}_n, \quad m_y = \frac{1}{N} \sum_i \mathbf{S}_i \cdot \hat{\mathbf{y}}_n, \quad (2)$$

where the orthogonal axes  $\hat{\mathbf{x}}_n \perp \hat{\mathbf{y}}_n$  on each site of a tetrahedron coincide with spin directions for the two states in Fig. 1. Our MC simulations measure statistical averages of  $m = (m_x^2 + m_y^2)^{1/2}$  and

$$m_6 = [(m_x + im_y)^6 + (m_x - im_y)^6]/(2m^5). \quad (3)$$

The total order parameter  $m$  gives the sublattice magnetization, whereas the clock-type order parameter  $m_6 = m \cos 6\theta$  distinguishes between  $\psi_2$  and  $\psi_3$  states: it is positive for the six non-coplanar  $\psi_2$  states,  $\theta_k = \pi k/3$ ,  $k = 0, \dots, 5$ , and negative for the coplanar  $\psi_3$  structures with  $\theta_k = \pi(1 + 2k)/6$ .

Figures 1(c) and 1(d) show the temperature dependence of the two order parameters for  $J_\perp^a = 0.5$  and 1. In each case the transition temperatures, denoted by vertical dashed lines were obtained from the crossing points of the Binder cumulants  $U_L = \langle m^4 \rangle / \langle m^2 \rangle^2$  for different cluster sizes  $L$ . We find the clock order parameter  $m_6$  to be positive confirming selection of the  $\psi_2$  state by thermal fluctuations.<sup>13,16</sup> However,  $m_6$  is strongly suppressed near  $T_c$  and grows as the system size increases at fixed  $T < T_c$ .

Scaling arguments<sup>31,33</sup> suggest the following finite size behavior of the two order parameters near the transition:

$$m = L^{-\beta/\nu} f(\tau L^{1/\nu}), \quad m_6 = L^{-\beta/\nu} g(\tau L^{1/\nu_6}), \quad (4)$$

where  $\tau = (T_c - T)/T_c$ . It is expected that  $m$  and  $m_6$  have the same critical exponent  $\beta$ , and a leading system

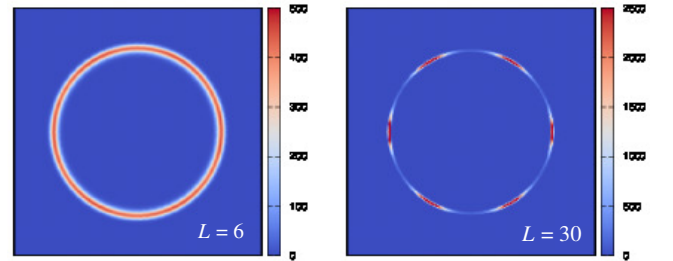


FIG. 2: (Color online) The distribution function  $P(m_x, m_y)$  for clusters with  $L = 6$  (left panel) and  $L = 30$  (right panel) measured at  $T = 0.5$  ( $J_\perp^a = 1$ ).

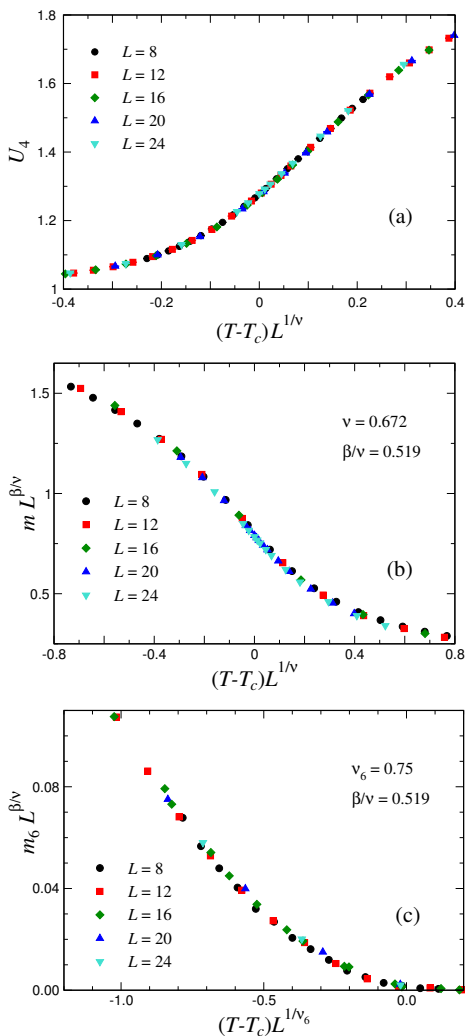


FIG. 3: (Color online) Finite-size scaling of the Monte Carlo data for the Binder cumulant  $U_L$  (a), the total order parameter  $m$  (b), and the clock order parameter  $m_6$  (c) using 3D XY critical exponents  $\beta$  and  $\nu$  with  $T_c = 0.4454$  ( $J_\perp^a = 0.5$ ).

size dependence in the critical region, scaling as  $L^{-\beta/\nu}$ . However, since the  $Z_6$  anisotropy is dangerously irrelevant in 3D one expects the scaling function to be controlled by a second divergent length scale: while the correlation length for  $m$  is  $\xi \sim |\tau|^{-\nu}$  with the standard XY value for  $\nu$ ,<sup>40</sup> the clock order parameter  $m_6$  only becomes nonzero above a larger length scale  $\xi_6 \sim |\tau|^{-\nu_6}$  with  $a_6 = \nu_6/\nu > 1$ . This new scale can be interpreted as a width of a domain wall between different  $\psi_2$  states. Inside the domain wall, the order parameter angle  $\theta$  smoothly varies and is not fixed to any discrete value. Consequently, MC simulations of clusters with  $L < \xi_6$  exhibit behavior typical of a  $U(1)$  symmetric model showing a finite value of  $m_6$  only once the cluster size  $L$  exceeds a temperature dependent scale  $\xi_6$ , see Figs. 1(c) and (d).

We illustrate the above behavior by showing in Fig. 2 histograms for the order parameter distribution  $P(m_x, m_y)$  obtained for  $J_\perp^a = 1$  on a small  $L = 6$  and a

large  $L = 30$  cluster at  $T = 0.5$  with  $T_c = 0.665$ . The radius of the distribution gives the average order parameter  $\langle m \rangle$  and does not change appreciably between the two clusters. The angular dependence of  $P(m_x, m_y)$  is, however, very different in the two cases. It is almost perfectly uniform for the small lattice, whereas the larger system exhibits pronounced peaks corresponding to the six domains of the  $\psi_2$  state.

*Critical exponents.*—The finite-size scaling hypothesis yields  $U_L = \tilde{f}(\tau L^{1/\nu})$  for the Binder cumulant near the transition,  $|\tau| \ll 1$ . Hence, detailed study of  $U_L$  allows to determine both  $T_c$  and  $\nu$ . Using small temperature steps and cluster sizes up to  $L = 24$  we have determined  $T_c = 0.4454(1)$  for  $J_\perp^a = 0.5$  (see the Supplemental Material for further details<sup>37</sup>). As shown in Fig. 3(a), an excellent data collapse is obtained for this value of  $T_c$  with  $\nu = 0.672$ , the best estimate for the 3D XY universality class.<sup>40</sup>

Further, Fig. 3(b), we find a very good collapse of the order parameter data plotted as  $mL^{\beta/\nu}$  vs.  $\tau L^{1/\nu}$ , with  $\beta/\nu = 0.519$ , corresponding to the 3D XY model:  $\beta = 0.348$  and from scaling relations,  $\eta = 0.038$ . In the Supplemental Material we present results of an alternative analysis, which independently confirm the estimates for  $\nu$  and  $\eta$  for this and other values of  $J_\perp^a$ .<sup>37</sup> Hence, the above results unambiguously establish that the transition occurring in the spin model for  $\text{Er}_2\text{Ti}_2\text{O}_7$  falls in the the 3D XY universality class.

A similar scaling analysis of the MC data for  $m_6$  allows to determine the extra exponent  $\nu_6$ . Using the standard value for  $\beta/\nu$  we obtain good data collapse for  $\nu_6 = 0.75(2)$  shown in Fig. 3(c). This value differs sharply from  $\nu_6 \approx 1.6$  obtained by Lou *et al.*,<sup>33</sup> who studied the XY model on a cubic lattice, perturbed by a hexagonal anisotropy. That is, the entropically driven 6-fold perturbation in the present model appears to be more dangerous than the corresponding energy perturbation. This is surprising, particularly so, given the observed small values for  $m_6$  compared to  $m$  near the transition, which confirms the weak nature of the entropic perturbation. Interestingly, our value of  $a_6 = \nu_6/\nu \approx 1.12$  appears to be closer to the value  $a_6 \approx 1.3$  found for an orbital model with the same  $Z_6$  symmetry.<sup>35</sup> In the Supplemental Material we present additional MC data for  $J_\perp^a = 1$ , which show that  $\nu_6$  does not change with a varying strength of the effective  $Z_6$  anisotropy.<sup>37</sup> Thus, the question of universality for the critical exponent  $\nu_6$  in different realizations of 3D  $Z_6$  models appears to be an open one.

*Neutron scattering.*—We now turn to the peculiar line shape for the magnetic Bragg peaks observed by Ruff *et al.*<sup>17</sup> in neutron diffraction experiments on  $\text{Er}_2\text{Ti}_2\text{O}_7$ . Measuring the elastic signal at  $T = 50$  mK in the vicinity of the (2,2,0) Bragg reflection, they found that the resolution limited peak indicative of true long-range magnetic order coexists with broad diffuse wings characteristic of short-range spin-liquid like correlations. The elastic scattering can be simulated within the static approximation

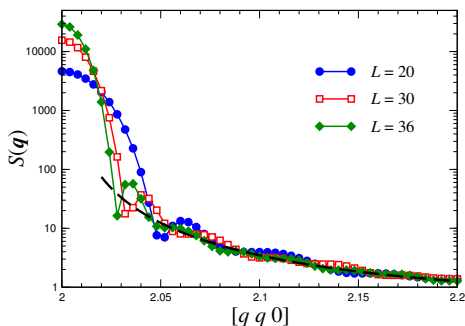


FIG. 4: (Color online) Magnetic structure factor in the vicinity of the (2,2,0) Bragg reflection obtained at  $T = 0.5$  for  $J_{\perp}^a = 1$ . The dashed line shows  $(q - 2)^{-2}$  fit for the diffuse scattering wing.

through the structure factor

$$S(\mathbf{q}) = \frac{1}{N} \sum_{i,j} e^{i\mathbf{q} \cdot (\mathbf{r}_i - \mathbf{r}_j)} \langle \mathbf{S}_i^{\perp} \cdot \mathbf{S}_j^{\perp} \rangle. \quad (5)$$

where  $\mathbf{S}_i^{\perp}$  now are spin components perpendicular to the wavevector. Equating this to the scattering function corresponds to setting the magnetic form factor equal to unity. In the following we adopt the standard convention for pyrochlore antiferromagnets, giving wavevectors in units of  $2\pi/a$ , where  $a$  is a linear size of the cubic cell containing 16 magnetic ions.

Figure 4 shows MC results for  $S(\mathbf{q})$  on a logarithmic scale in the vicinity of the  $\mathbf{Q} = (2, 2, 0)$  reflection obtained at  $T = 0.5$  for  $J_{\perp}^a = 1$  on three large clusters. The Bragg peak has a width  $\propto 1/L$ . After a pronounced dip, the magnetic structure factor displays a few damped finite-size oscillations with period  $\Delta\mathbf{q} = 1/L$ . Besides that  $S(\mathbf{q})$  has a finite diffuse component, which gradually decreases with the distance from the Bragg peak. The intensity in the scattering wing follows a power law  $S(\mathbf{Q} + \mathbf{q}) \sim 1/q^n$  with  $n \approx 2$ . The corresponding fit is shown by a dashed line in Fig. 4.

This general behavior closely resembles the experimental profile of the (2,2,0) peak in  $\text{Er}_2\text{Ti}_2\text{O}_7$ .<sup>17</sup> Additional MC simulations included in Supplemental Material<sup>37</sup> show that the form of the diffuse scattering wings is maintained as the temperature is lowered but that the intensity is reduced by a factor of 4 between  $T = 0.5$

and  $T = 0.3$  ( $T_c = 0.636$ ). The persistence of the diffuse scattering is consistent with the phenomenon of order stabilized through fluctuations, with the temperature dependence being indicative of a thermal process. In contrast, the anomalous intensity wings have been observed experimentally at  $T = 50 \text{ mK} \ll T_N$ . We interpret this as a manifestation of the quantum dynamics, which are present in the original effective spin-1/2 model (1) for  $\text{Er}_2\text{Ti}_2\text{O}_7$ , providing evidence that, at low temperature the order is indeed maintained by quantum fluctuations, as has been previously proposed.<sup>11,13,14</sup> Finally, we remark that a similar profile for the Bragg peaks was observed in  $\text{Tb}_2\text{Sn}_2\text{O}_7$ ,<sup>41</sup> in which ferromagnetically aligned  $z$  components of magnetic ions coexist with antiferromagnetic ordering of transverse components.

*Conclusions.*—The model of anisotropic  $XY$  pyrochlore antiferromagnet has been shown to reproduce essentially all experimental features of the frustrated magnetic material,  $\text{Er}_2\text{Ti}_2\text{O}_7$ , including a second order phase transition to the 6-fold symmetric  $\psi_2$  state, driven by an order by disorder mechanism. Our extensive Monte Carlo simulations provide convincing evidence that the transition falls into the universality class of an emergent  $XY$  symmetry. The underlying discrete symmetry manifests itself at the transition as a dangerously irrelevant scaling variable. The scaling is found to be more dangerous than in the previously studied case of energetic perturbation,<sup>31,33</sup> despite a very weak onset of 6-fold ordering in the critical region. Future work could investigate the role of entropic forces for this apparently non-universal dangerous irrelevance by, for example, studying a clock model with the same Hamiltonian. Simulated neutron scattering patterns below the transition show the coexistence of both Bragg peaks and an extensive background of diffuse scattering characteristic of spin liquid behavior in good agreement with experiment. While in the experiment the diffuse scattering persists down to low temperature, it weakens in our classical system providing evidence of the presence of extensive quantum fluctuations in  $\text{Er}_2\text{Ti}_2\text{O}_7$ .

We are grateful to M. J. P. Gingras and P. Dalmas de Réotier for useful discussions and to M. V. Gvozdkova for help with Monte Carlo simulations. MEZ and PCWH acknowledge hospitality of the Max Planck Institute for the Physics of Complex Systems, where part of this work was performed.

- <sup>1</sup> M. J. Harris, S. T. Bramwell, D. F. McMorrow, T. Zeiske, and K. W. Godfrey, *Phys. Rev. Lett.* **79**, 2554 (1997).
- <sup>2</sup> R. Coldea, D. A. Tennant, A. M. Tsvelik, and Z. Tylczynski, *Phys. Rev. Lett.* **86**, 1335 (2001).
- <sup>3</sup> M. A. de Vries, J. R. Stewart, P. P. Deen, J. O. Piatek, G. J. Nilsen, H. M. Ronnow, and A. Harrison, *Phys. Rev. Lett.* **103**, 237201 (2009).
- <sup>4</sup> T.-H. Han, J. S. Helton, S. Chu, D. G. Nocera, J. A. Rodriguez-Rivera, C. Broholm, and Y. S. Lee, *Nature* **492**,

406 (2012).

- <sup>5</sup> H. Kageyama, K. Onizuka, Y. Ueda, N. V. Mushnikov, T. Goto, K. Yoshimura, and K. Kosuge, *Phys. Rev. Lett.* **82**, 3168 (1999).
- <sup>6</sup> H. Ueda, H. A. Katori, H. Mitamura, T. Goto, and H. Takagi, *Phys. Rev. Lett.* **94**, 027202 (2005).
- <sup>7</sup> N. A. Fortune, S. T. Hannahs, Y. Yoshida, T. E. Sherline, T. Ono, H. Tanaka, and Y. Takano, *Phys. Rev. Lett.* **102**, 257201 (2009).

- <sup>8</sup> J. R. Stewart, G. Ehlers, A. S. Wills, S. T. Bramwell, and J. S. Gardner, *J. Phys. Condens. Matter* **16**, L321 (2004).
- <sup>9</sup> M. Tamura, A. Nakao, and R. Kato, *J. Phys. Soc. Jpn.* **75**, 093701 (2006).
- <sup>10</sup> M. Mourigal, M. Enderle, B. Fåk, R. K. Kremer, J. M. Law, A. Schneidewind, A. Hiess, and A. Prokofiev, *Phys. Rev. Lett.* **109**, 027203 (2012).
- <sup>11</sup> J. D. M. Champion, M. J. Harris, P. C. W. Holdsworth, A. S. Wills, G. Balakrishnan, S. T. Bramwell, E. Cizmar, T. Fennell, J. S. Gardner, J. Lago, D. F. McMorrow, M. Orendac, A. Orendacova, D. McK. Paul, R. I. Smith, M. T. F. Telling, and A. Wildes, *Phys. Rev. B* **68**, 020401(R) (2003).
- <sup>12</sup> A. Poole, A. S. Wills, and E. Lelièvre-Berna, *J. Phys.: Condens. Matter* **19**, 452201 (2007).
- <sup>13</sup> M. E. Zhitomirsky, M. V. Gvozdkova, P. C. W. Holdsworth, and R. Moessner, *Phys. Rev. Lett.* **109**, 077204 (2012).
- <sup>14</sup> L. Savary, K. A. Ross, B. D. Gaulin, J. P. C. Ruff, and L. Balents, *Phys. Rev. Lett.* **109**, 167201 (2012).
- <sup>15</sup> S. T. Bramwell, M. J. P. Gingras, and J. N. Reimers, *J. Appl. Phys.* **76**, 5523 (1994).
- <sup>16</sup> J. D. M. Champion and P. C. W. Holdsworth, *J. Phys.: Condens. Matter* **16**, S665 (2004).
- <sup>17</sup> J. P. C. Ruff, J. P. Clancy, A. Bourque, M. A. White, M. Ramazanoglu, J. S. Gardner, Y. Qiu, J. R. D. Copley, M. B. Johnson, H. A. Dabkowska, and B. D. Gaulin, *Phys. Rev. Lett.* **101**, 147205 (2008).
- <sup>18</sup> S. S. Sosin, L. A. Prozorova, M. R. Lees, G. Balakrishnan, and O. A. Petrenko, *Phys. Rev. B* **82**, 094428 (2010).
- <sup>19</sup> H. B. Cao, I. Mirebeau, A. Gukasov, P. Bonville, and C. Decorse, *Phys. Rev. B* **82**, 104431 (2010).
- <sup>20</sup> S. Onoda and Y. Tanaka, *Phys. Rev. Lett.* **105**, 047201 (2010).
- <sup>21</sup> K. A. Ross, L. Savary, B. D. Gaulin, and L. Balents, *Phys. Rev. X* **1**, 021002 (2011).
- <sup>22</sup> O. A. Petrenko, M. R. Lees, and G. Balakrishnan, *J. Phys.: Condens. Matter* **23**, 164218 (2011).
- <sup>23</sup> P. Dalmas de Réotier, A. Yaouanc, Y. Chapuis, S. H. Curnoe, B. Grenier, E. Ressouche, C. Marin, J. Lago, C. Baines, and S. R. Giblin, *Phys. Rev. B* **86**, 104424 (2012).
- <sup>24</sup> P. Bonville, S. Petit, I. Mirebeau, J. Robert, E. Lhotel, and C. Paulsen, *J. Phys.: Condens. Matter* **25**, 275601 (2013).
- <sup>25</sup> N. R. Hayre, K. A. Ross, R. Applegate, T. Lin, R. R. P. Singh, B. D. Gaulin, and M. J. P. Gingras, *Phys. Rev. B* **87**, 184423 (2013).
- <sup>26</sup> A. W. C. Wong, Z. Hao, and M. J. P. Gingras, *Phys. Rev. B* **88**, 144402 (2013).
- <sup>27</sup> J. Oitmaa, R. R. P. Singh, B. Javanparast, A. G. R. Day, B. V. Bagheri, and M. J. P. Gingras, *Phys. Rev. B* **88**, 220404 (2013).
- <sup>28</sup> P. A. McClarty, P. Stasiak, and M. J. P. Gingras, *Phys. Rev. B* **89**, 024425 (2014).
- <sup>29</sup> K. A. Ross, Y. Qiu, J. R. D. Copley, H. A. Dabkowska, and B. D. Gaulin, *Phys. Rev. Lett.* **112**, 057201 (2014).
- <sup>30</sup> D. Blankschtein, M. Ma, A. N. Berker, G. S. Grest, and C. M. Soukoulis, *Phys. Rev. B* **29**, 5250 (1984).
- <sup>31</sup> M. Oshikawa, *Phys. Rev. B* **61**, 3430 (2000).
- <sup>32</sup> J. Hove and A. Sudbo, *Phys. Rev. E* **68**, 046107 (2003).
- <sup>33</sup> J. Lou, A. W. Sandvik, and L. Balents, *Phys. Rev. Lett.* **99**, 207203 (2007).
- <sup>34</sup> G.-W. Chen, [arXiv:1008.3038](https://arxiv.org/abs/1008.3038).
- <sup>35</sup> S. Wenzel and A. M. Läuchli, *Phys. Rev. Lett.* **106**, 197201 (2011).
- <sup>36</sup> S. H. Curnoe, *Phys. Rev. B* **78**, 094418 (2008).
- <sup>37</sup> see the Supplemental Material.
- <sup>38</sup> M. Creutz, *Phys. Rev. D* **36**, 515 (1987).
- <sup>39</sup> M. E. Zhitomirsky, *Phys. Rev. B* **78**, 094423 (2008).
- <sup>40</sup> M. Campostrini, M. Hasenbusch, A. Pelissetto, and E. Vicari, *Phys. Rev. B* **74**, 144506 (2006).
- <sup>41</sup> Y. Chapuis, A. Yaouanc, P. Dalmas de Réotier, S. Pouget, P. Fouquet, A. Cervellino, and A. Forget, *J. Phys.: Condens. Matter* **19**, 446206 (2007).